Published in final edited form as:
Neuroinformatics. 2008 ; 6(2): 71–79. doi:10.1007/s12021-008-9013-2.

Phylogenetic proximity revealed by neurodevelopmental event timings

Radhakrishnan Nagarajan[1] and **Barbara Clancy**[2]

[1]Department of Biostatistics, University of Arkansas for Medical Sciences, COPH/UAMS, Room 3234, 4301 W Markham, Slot 781, Little Rock, AR 72205-7199, Tel: 501-526-6734, Fax: 501-526-6729, Email: nagarajanradhakrish@uams.edu

[2]Department of Biology, University of Central Arkansas, Conway, Arkansas 72035

Abstract

Statistical properties such as distribution and correlation signatures were investigated using a temporal database of common neurodevelopmental events in the three species most frequently used in experimental studies, rat, mouse, and macaque. There was a fine nexus between phylogenetic proximity and empirically derived dates of the occurrences of 40 common events including the neurogenesis of cortical layers and outgrowth milestones of developing axonal projections. Exponential and power-law approximations to the distribution of the events reveal strikingly similar decay patterns in rats and mice when compared to macaques. Subsequent hierarchical clustering of the common event timings also captures phylogenetic proximity, an association further supported by multivariate linear regression data. These preliminary results suggest that statistical analyses of the timing of developmental milestones may offer a novel measure of phylogenetic classifications. This may have added pragmatic value in the specific support it offers for the reliability of rat/mouse comparative modeling, as well as in the broader implications for the potential of meta-analyses using databases assembled from the extensive empirical literature.

Keywords

comparative neural development; cross-species modeling; macaque; mouse; neuroinformatics; phylogeny; rat

1. Introduction

Although neurodevelopment occurs at dissimilar times and intervals in different mammalian species, it consists of similar events and follows remarkably conserved sequences (1). For example, rats have a gestational period of 21.5 days, compared to 165 days for macaques, yet in both species ganglion cells in the retina are generated (“born”) before amacrine cells, neurons that form the cortical subplate are generated prior to neurons of the cortical laminae, and axons projecting from the retina reach the optic chiasm long before they segregate into ipsilateral and contralateral patterns in the lateral geniculate nucleus. Identification of statistical relationships in the timing of such developmental milestones (neural “events”) across various mammalian species has proved useful in understanding general concepts about evolution and development (2,3), and has been applied in a pragmatic fashion to extrapolate data obtained from well-

Correspondence to: Radhakrishnan Nagarajan.

Information Sharing Statement: The general public can access relevant databases, references, and citation information at http://www.translatingtime.net/. A table (Table I) is enclosed as a part of the manuscript containing the data used in the present study.

studied experimental species to humans (4–6). Recently, a database of events gleaned from the published literature, including a predictive application, was made available at http://www.translatingtime.net/ (7).

The present study systematically investigates the fine nexus between the statistical properties of common neurodevelopmental event timings obtained from this database, and phylogenetic proximity. A sufficient number of neurodevelopmental event dates (40) have been established in three species, namely: *Rattus Norvegicus* (rat), *Mus Musculus* (mouse), classified as *rodents*, and the *primate Macaca Mulatta* (macaque) to warrant such analysis. We find exponential and power-law approximations (8,9) to the distribution of the common events exhibit considerable similarity between mouse and rat, yet are different from the macaque pattern, reflecting the rodents' phylogenetic proximity. The decay of the distribution is relatively faster in both rodents when compared to macaque. Hierarchical clustering (10) of the common events across the three mammals, and subsequent prediction of the events using multivariate linear regression (10,11) also captures the phylogenetic proximity. These statistical similarities suggest that the timing of developmental milestones may offer a novel measure of phylogenetic classifications. The similarities between rat and mouse also have pragmatic value in that they serve to bolster existing conversions (http://www.translatingtime.net/). This is of particular value as the vast previous neurodevelopmental studies accomplished in rat now require conversion to the newly favored mouse.

2. Data

Over the course of several previous studies (1,4,7,12), the timing of 102 early neurodevelopmental events (i.e. dates in central nervous system development that occur less than 160 days post-conception (PC) in humans) were systematically collected from the empirical literature on ten mammalian species. Events are defined as empirically derived occurrences in brain development, such as when neurons destined for various cortical layers are born (neurogenesis dates) and milestones in fiber tract outgrowth. These data were obtained from the general literature (13–24) including from published tables compiled by several authors (1,25–27,35). Dates following conception reported in the empirical literature were converted where necessary such that first 24-hour period post conception is always designated post conceptional day (PC) 1.

Our dataset is based on an earlier version established by Finlay and Darlington (1), who used it to define evolutionary principles. We sought to ensure as much consistency as possible in our database, but it should be noted that compilation of data across laboratories, no matter how carefully the original studies were done, will always introduce some amount of error in standardization, and some degree of variability. Our database consists of empirical observations published by many different researchers reporting the timing of milestones in brain development, with studies typically accomplished in several animals and reported by the authors as averages. Although developmental processes are typically continuous, we used consistent and clearly reported start and stop dates whenever available. However some data, neurogenesis dates for example, are sometimes reported in histograms. When converting from histograms, we assigned a "start" date as the day on which 5% of the neurons of a given structure were generated; with "end" defined similarly. Assigning dates for axon growth presented a different problem as these type events can only be reported when they are observed, and are thus subject to a sampling delay error that is dependent on the original sampling intervals. Yet despite the inherent difficulties, meta-analyses of such data have been used successfully in many previous studies (1,5,12,25–27,35). Additional details on the data used in this study are publicly available, with references, at http://www.translatingtime.net (7).

The largest number of event dates was collected in three species; 74 events in the developing rat brain, 91 events in mouse and 66 events in macaque. Across the three species, a total of 40 of these were common events, a number that proved sufficient for the analyses we describe here. All of the 40 common neural milestones can be considered "progressive" events; 34 are post conception (PC) days for the start, peak, or end of neurogenesis for various brain regions including subcortical nuclei, retinal cells, and cortical laminae, five are dates related to the appearance of fiber tracts, and the last (1,4,7,12) is the final milestone in the current data base, the day eye-opening occurs. Table I lists the 40 events along with their timing, mean, and standard deviation. Corresponding references can be found at http://bioinformatics.ualr.edu/ttime/relatedtables.php.

3. Analyses and Results

3.1 Power-law and exponential approximations to the distribution of the common events

The probability of occurrence of the events P(k) as function of their magnitude (k) across these three mammals is shown in Figs. 1a, 1b and 1c respectively. Kolmogorov-Smirnov (KS) goodness of fit (28) was used for pair-wise comparison of the distributional signatures across the three mammals. Pair-wise comparison of the distribution of the 40 common events between mouse and rat failed to reject the null hypothesis that the distributions of the events are drawn from the same underlying distribution ($p < 0.001$). However, in similar comparisons between rats and macaque, as well as mouse and macaque, the null hypothesis was rejected ($p < 0.001$). While KS is useful is establishing the phylogenetic proximity, it is sensitive to the average event timing. The distribution of the 40 common events across the three species is skewed to the left indicating that the frequency of occurrence of neurodevelopmental events P(k) exhibits a decaying trend with increasing (k), Fig. 1. Such a behavior was consistent across the three mammals. The present study uses two popular parametric distributions, namely: exponential and power-law approximations to capture the decaying trend. The term approximation is used purposely in order to acknowledge finite-size effects inherent in such studies. While both exponential, $P(k) = \beta_e e^{-\gamma_e k}$, and power-law distributions $P(k) = \beta_p k^{-\gamma_p}$, exhibit a decaying trend, there are subtle yet significant statistical differences between these two classes of distributions.

Consider an exponentially distributed random variable ($\tilde{k}$) with $P(\tilde{k} > k) = e^{-\gamma_e k}$, we have

$$\mathrm{P}\left(\tilde{k}>k_1+k_2 \mid \tilde{k}>k_2\right)=\frac{e^{-\gamma_e(k_1+k_2)}}{e^{-\gamma_e k_2}}=e^{-\gamma_e k_1}=P\left(\tilde{k}>k_1\right).$$

i.e. the future is conditionally independent of the past, hence memoryless. However, for a power-law distributed variable ($\tilde{k}$) with $P(\tilde{k} > k) = k^{-\gamma_p}$, we have

$$\mathrm{P}\left(\tilde{k}>k_1+k_2 \mid \tilde{k}>k_2\right)=\frac{(k_1+k_2)^{-\gamma_p}}{k_2{}^{-\gamma_p}}=(1+\frac{k_1}{k_2})^{-\gamma_p} \neq P\left(\tilde{k}>k_1\right)$$

i.e. the future is **not** conditionally independent of the past, hence **not** memoryless.

In either case, the decay of the distribution is directly proportional to the magnitude of the exponents (γ_p, γ_e). Prior to determining the exponents (γ_p, γ_e) the expression for the power-law and exponential distributions were linearized as follows

$$\log P(k) = \log(\beta_p) - \gamma_p \log(k) \quad (1)$$

$$\log P(k) = \log(\beta_e) - \gamma_e k \quad (2)$$

The number of bins in the histogram which represents the number of points in the regression of (1) and (2) was chosen approximately as the square root of the number of events, i.e. $\sqrt{40} \sim 6$. A value of one was added to *P(k)* to ensure non-zero frequency and existence of the log-transform in expressions (1) and (2). Linear regression of the events distributions across mouse, rat and macaque using power-law model (1) resulted in (γ_p = 3.3, 3.2 and 2.5) in that order, Figs. 1d, 1e and 1f. A similar analysis using the exponential model (2) resulted in (γ_e = 0.16, 0.14 and 0.04), Figs. 1g, 1h and 1i. Visual inspections of Fig. 1 reveal both the exponential as well as power-law models as plausible approximations to the events distributions across the mammals. However, it is prudent to *validate* the fit using well-defined measures in the case of competing models explaining the same data. Prior to validation it is important to note that the number of parameters across the two models and the number of samples used in the linear regression were the same. Thus there is no need to incorporate sophisticated statistics to accommodate the variation in the number of parameters or the number of data points in the validation criteria. In the present study we used R^2 statistics [29] and the Akaike information criterion (AIC) [30, 31] to validate the fit. Using a combination of validation criteria rejects the claim that the conclusions drawn are based on the assumptions of a particular validation criterion. While R^2 represents the percentage of variance in the given data explained by the regression model, AIC is an information theoretic criterion which relies on the popular formulation of Occam's razor. The larger the value of R^2, the better the fit can be used to explain the given data. This is in sharp contrast with AIC, which results in lower values for better fits. The R^2 for the power-law model (1) across mouse, rat and macaque was (R^2 = 0.78, 0.60 and 0.85) in that order, whereas for the exponential model (2) was (R^2 = 0.72, 0.60 and 0.84). Similar analysis using AIC as the validation criterion resulted in (AIC = 15.9, 21.3, 12.9) for the power-law model (1) and (AIC = 17.2, 22.6, 13.2) for the exponential model (2). Given inherent finite size effects and insignificant change in AIC and R^2 values, we believe either of these models can be used to explain the distributional signatures of the common events across the three species. It is important to note that the magnitude of the exponent of the power-law (γ_p) as well as exponential (γ_e) approximation reflects the phylogenetic proximity between these species. The magnitude of the exponents in macaque (γ_p = 3.3, γ_e = 0.16) was considerably lower than those of mouse (γ_p = 3.2, γ_e = 0.14) and rat (γ_p = 2.5, γ_e = 0.04) indicating relatively slower decay in the event timings during neurodevelopment in macaque.

3.2 Hierarchical clustering of the common events across the three species

The 40 common events across the three species were hierarchically classified using linear correlation metric and complete linkage [10]. It is important to validate the dendrogram representation with respect to the given data, i.e. faithfulness of the hierarchical representation in capturing the dissimilarities between the three species. A popular metric used to accomplish above is the cophenetic correlation coefficient (ψ) [32–34], which is basically the linear correlation between the cophenetic distances obtained from the dendrogram and the actual dissimilarities used to construct the dendrogram (Mathworks, Natick, MA). Hierarchical clustering of the 40 common events indicated significant proximity between mouse and rat as opposed to macaque with (ψ = 0.99) reflecting their phylogenetic proximity (see Fig. 2). Biological significance of the results generated by hierarchical clustering across the events was unclear.

3.3 Multivariate linear regression of the common events across the three species

Multivariate linear regression is used widely to predict the *response* variable using a given set of *predictor* variables [10, 11]. The weights of the predictors represent the relative contribution

in predicting the unknown variable. Since there are three species in the present study, the third species can be predicted as a linear combination of the other two. There are three possible cases (i) predict mouse events using information of rat and macaque events; (ii) predict rat events using information of mouse and macaque events; (iii) predict macaque events using information of mouse and rat events. Preliminary investigation using the 40 common events across the three species yielded the following: (i) relative contribution of rat and macaque in predicting mouse events were (0.80 and 0.02) respectively. The weights of the regression coefficients reflect considerable significant contribution from rat as opposed to macaque in predicting mouse events. (ii) Relative contribution of mouse and macaque in predicting rat events were (1.0 and 0.03) respectively. As in (i), the weights of the regression coefficients reflect considerable significant contribution from mouse as opposed to macaque in predicting rat events. (iii) The relative contribution of mouse and rat in predicting macaque events were (1.7 and 1.8) respectively. Unlike (i) and (ii), the weights of the regression coefficients indicate minimal discrepancy in the contribution of mouse and rat in predicting macaque events.

In order to further establish the connection between the regression weights and phylogenetic proximity we followed a bootstrap approach. In the present context, the 40 common events across the species were thought to be representative of the population. Subsequently, 20 common events across the three species were bootstrapped independently from these 40 events by resampling without replacement. The distribution of the relative contribution of the regression weights of the predictor variables across 500 independent bootstrap realizations for case (i) is shown in Figs. 3a and 3b respectively. Those for cases (ii) and (iii) are shown in Figs. 3c, 3d, and 3e, 3f, respectively. The confidence limit for 15 bootstrap realizations across the three cases is shown in Fig. 4. The distribution of the weights, Fig. 3, clearly reflects the phylogenetic proximity between rat and mouse.

4. Discussion

Despite the complexity of the various systems involved in development of the central nervous system, statistical analyses can be used to characterize similarities and differences in the timing of neural developmental events across mammalian species. The present study investigated statistical properties including exponential and power-law approximations, hierarchical clustering and multivariate linear regression data using a database gleaned from the empirical literature of 40 common neurodevelopmental events across mouse, rat and macaque.

4.1 Modeling phylogenetic proximity

Mathematics and statistical methods, including hierarchical clustering are the cornerstones of phylogenetic classifications whether used to sort by traditional methods such as genes and proteins, or less conventional items such as behavior (11) or brain traits (12). We suggest that statistical analysis of the timing of neural development also may offer a novel measure of phylogenetic classifications into species' phylogenetic proximity as: (a) phylogenetic proximity between species can be captured by the parameters of power-law as well as by exponential approximations (b) hierarchical clustering of the 40 common neurodevelopmental event timings using correlation metric reflect the phylogenetic proximity between the species, with faithfulness established by the cophenetic correlation coefficient. (c) regression coefficients also reflect the phylogenetic proximity between the species, with rats contributing to the prediction of mouse events and vice-versa.

Validation of the power-law and the exponential approximations using classical linear regression statistics (R^2, AIC) revealed the close relationship between rat and mouse neural development, did the weights of the multivariate linear regression coefficients which implicitly reflect the phylogenetic proximity between the species. The distributional signatures of the 40 common events across all three species exhibited a decaying trend, with distribution signatures

skewed to the left, indicating that the frequency of occurrence of neurodevelopmental events P(*k*) exhibits a decaying trend with increasing (*k*). Yet mouse and rat distributions show a considerable similarity as reflected by the distributional parameters. Subsequent hierarchical clustering of the common events using correlation metric and complete linkage also reflected the rodent phylogenetic proximity.

It should be noted that although we emphasize rat/mouse similarities due to what this seems to indicate about phylogenetic classifications, the distributional signatures of the 40 common events demonstrate considerable similarity across all three species. This is in accord with many previous studies that report striking similarities in the manner in which mammalian brains develop [1, 5, 11, 25–27, 37].

4.2 Phylogenetic proximity strongly supports rat/mouse conversions

Over the course of the past years, considerable empirical data have been generated regarding rat neural development, although less have been collected in mice (22). Yet recent National Institutes of Health (NIH) initiatives assign a new high priority to mouse resources, based on the explosion of genomic studies now accomplished or planned in mice. The murine emphasis compels researchers to identify how to best equate neurodevelopmental events that occur in rats (gestation averages 21.5 days) to similar events in mice (gestation averages 18.5 days). The answer lies on a spectrum ranging from simply subtracting the 3 days difference in gestation time to requiring that the abundant studies done over so many years in rat models be repeated in mice.

We strongly suggest that the problem can be addressed, and thus solutions better understood, using neuroinformatics principles, including methods used in this study. Because multivariate regression can be used to establish the phylogenetic proximity of the two rodent species from the weights of the regression coefficients, we are able to conclude that rat neurodevelopment event timing can play an important role in predicting mouse event timing, and vice-versa. On the other hand, the magnitude of the decay exponents (γ_p, γ_e) indicates that macaques exhibit considerably slower decay than rodents, likely reflecting the longer and more complex nature of neurodevelopment programs in primates. The delay likely reflects the elongation of the neural development window. Macaque gestation is approximately three times that of rodents (165 days), and although not true measure of total brain development time, it reflects the additional time to complete brain maturation in primates. The close relationship in the two rodents suggests previous mathematical extrapolations between these two species are likely to be particularly reliable, supporting use of our comparative dataset available at http://www.translatingtime.net. The value of such support lies in increased assurance that such translational modeling may possibly encourage investigators to target a limited, specific range of time points for their studies across species.

Acknowledgements

This project was partially supported by NIH Grant Number P20 RR-16460 from the IDeA Networks of Biomedical Research Excellence (INBRE) Program of the National Center for Research Resources. The authors would like to thank Susan Lantz for helpful comments and suggestions on an earlier version of this manuscript.

Reference

1. Finlay BL, Darlington RB. Linked regularities in the development and evolution of mammalian brains. Science 1995;268:1578–1584. [PubMed: 7777856]
2. Finlay BL, Darlington RB, Nicastro N. Developmental structure in brain evolution. Behavioral and Brain Sciences 2001;24:263–307. [PubMed: 11530543]

3. Clancy, B.; Finlay, B. Essential Readings in Language Development. Amsterdam: Elsevier; 2003. Neural Correlates of Early Language Learning.
4. Clancy B, Darlington RB, Finlay BL. The course of human events: predicting the timing of primate neural development. Developmental Science 2000;3:57–66.
5. Clancy B, Darlington RB, Finlay BL. Translating developmental time across mammalian species. Neuroscience 2001;105:7–17. [PubMed: 11483296]
6. Clancy B. Practical use of evolutionary neuroscience principles. Behavioral and Brain Sciences 2006;29:14–15.
7. Clancy B, Kersh B, Hyde J, Darlington RB, Anand KJ, Finlay BL. Web-based method for translating neurodevelopment from laboratory species to humans. Neuroinformatics 2007;5:79–94. [PubMed: 17426354]
8. Stanley HE. Power laws and Universality. Nature 1995;378:554.
9. Newman MEJ. Power-laws, Pareto Distributions and Zipf's law. Contemporary Physics 2005;46:323.
10. Jobson, JD. Applied Multivariate Data Analysis: Vol. II: Categorical and Multivariate Methods. Springer-Verlag; 1992.
11. Darlington, RB. Regression and Linear Models. McGraw-Hill; 1990.
12. Darlington RB, Dunlop SA, Finlay BL. Neural development in metatherian and eutherian mammals: variation and constraint. J Comp Neurol 1999;411:359–368. [PubMed: 10413772]
13. Bayer SA, Altman J. Development of layer I and the subplate in the rat neocortex. Exp Neurol 1990;107(1):48–62. [PubMed: 2295319]
14. Bayer, SA.; Altman, J. Neocortical development. Vol. xiv. New York: Raven Press; 1991. p. 255
15. Brunjes PC, Korol DL, Stern KG. Prenatal neurogenesis in the telencephalon of the precocial mouse Acomys cahirinus. Neurosci Lett 1989;107(1–3):114–119. [PubMed: 2616023]
16. Caviness VS Jr. Neocortical histogenesis in normal and reeler mice: a developmental study based upon [3H]thymidine autoradiography. Brain Res 1982;256(3):293–302. [PubMed: 7104762]
17. Kostovic I, Rakic P. Cytology and time of origin of interstitial neurons in the white matter in infant and adult human and monkey telencephalon. J Neurocytol 1980;9(2):219–242. [PubMed: 7441294]
18. Langford C, Sefton AJ. The relative time course of axonal loss from the optic nerve of the developing guinea pig is consistent with that of other mammals. Vis Neurosci 1992;9(6):555–564. [PubMed: 1450107]
19. Luskin MB, Shatz CJ. Neurogenesis of the cat's primary visual cortex. J Comp Neurol 1985;242(4): 611–631. [PubMed: 4086673]
20. Meister M, Wong RO, Baylor DA, Shatz CJ. Synchronous bursts of action potentials in ganglion cells of the developing mammalian retina. Science 1991;252(5008):939–943. [PubMed: 2035024]
21. Price DJ, Blakemore C. Regressive events in the postnatal development of association projections in the visual cortex. Nature 1985;316:721–724. [PubMed: 3839903]
22. Rakic P. Neurons in rhesus monkey visual cortex: systematic relation between time of origin and eventual disposition. Science 1974;183(123):425–427. [PubMed: 4203022]
23. Woo TU, Beale JM, Finlay BL. Dual fate of subplate neurons in a rodent. Cereb Cortex 1991;1(5): 433–443. [PubMed: 1822751]
24. Zhou ZJ. Direct participation of starburst amacrine cells in spontaneous rhythmic activities in the developing mammalian retina. J Neurosci 1998;18(11):4155–4165. [PubMed: 9592095]
25. Robinson SR, Dreher B. The visual pathways of eutherian mammals and marsupials develop according to a common timetable. Brain Behav Evol 1990;36(4):177–195. [PubMed: 2279233]
26. Ashwell KW, Waite PM, Marotte L. Ontogeny of the projection tracts and commissural fibres in the forebrain of the tammar wallaby (Macropus eugenii): timing in comparison with other mammals. Brain Behav Evol 1996;47(1):8–22. [PubMed: 8834781]
27. Dunlop SA, Tee LB, Lund RD, Beazley LD. Development of primary visual projections occurs entirely postnatally in the fat-tailed dunnart, a marsupial mouse, Sminthopsis crassicaudata. J Comp Neurol 1997;384(1):26–40. [PubMed: 9214538]
28. Press, WH.; Flannery, BP.; Teukolsky, SA.; Vetterling, WT. Numerical Recipes in FORTRAN: The Art of Scientific Computing. Vol. 2nd ed.. Cambridge, England: Cambridge University Press; 1992. p. 617-620.

29. Harrell, FE. Regression Modeling Strategies. Springer N.Y.: 2001.

30. Akaike, H. Information theory and an extension of the Maximum Likelihood Principle; Proceedings of the 2nd International Symposium of Information Theory; Akadamiai Kiado, Budapest. 1973. p. 267-281.

31. Hurvich CM, Tsai CL. Regression and time series model selection in small samples. Biometrika 1989;76:297–307.

32. Romesburg, HC. Cluster Analysis for Researchers. Belmont, CA: Lifetime Learning Publications; 1984.

33. Everitt, B. Cluster Analysis. Vol. 3rd edn.. London: Edward Arnold; 1993.

34. Tamayo P, Scanfeld D, Ebert BL, Gillette MA, Roberts CW, Mesirov JP. Metagene projection for cross-platform, cross-species characterization of global transcriptional states. Proc Natl Acad Sci U S A 2007;104(14):5959–5964. [PubMed: 17389406]

35. Clancy B, Finlay BL, Darlington RB, Anand KJ. Extrapolating brain development from experimental species to humans. Neurotoxicology 2007;28:931–937. [PubMed: 17368774]

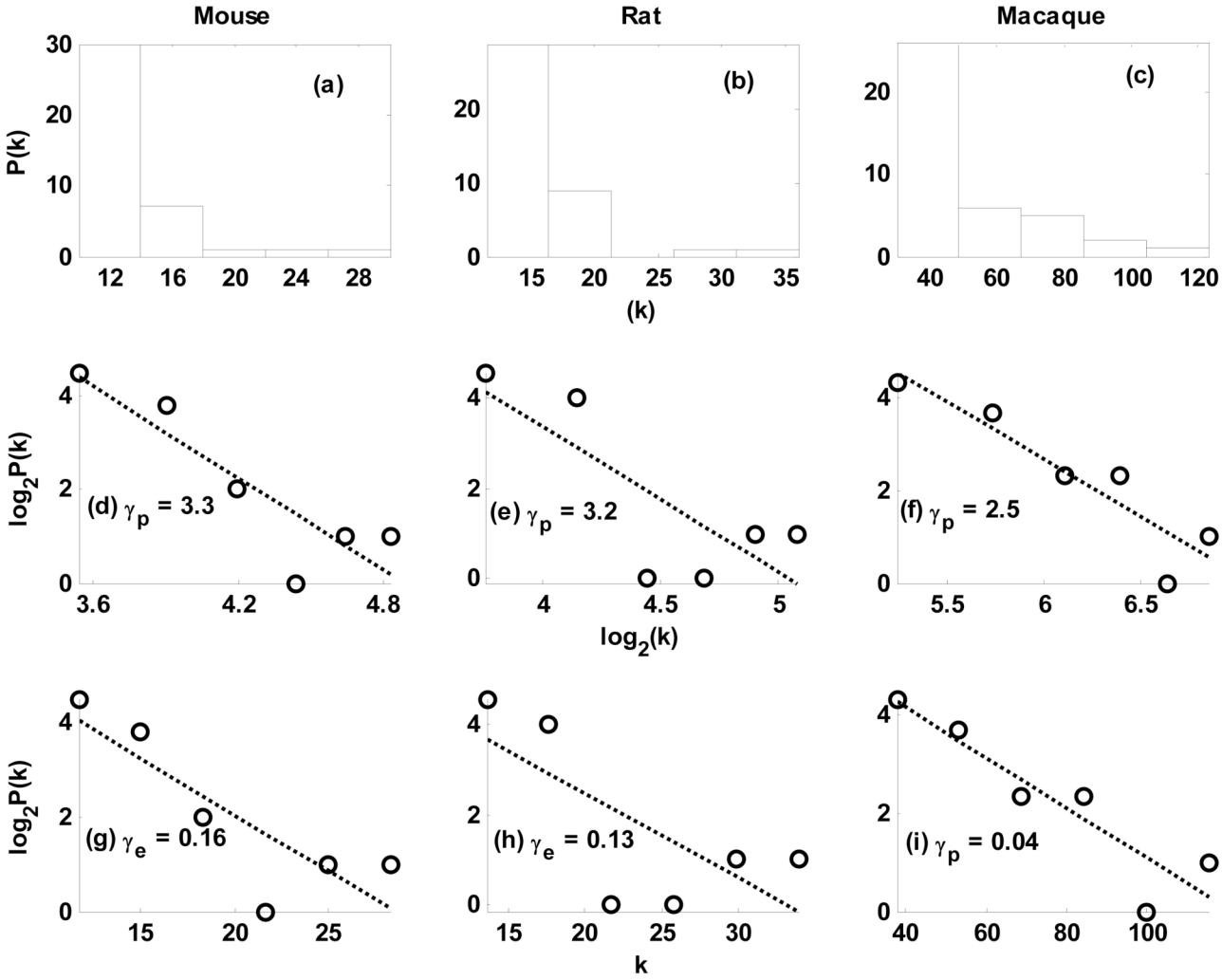

Figure 1.

Histogram representing the frequency of occurrence P(*k*) of the events (*k*) across mouse, rat and macaque is shown in (a, b and c) respectively. Power-law approximation to the distributions (a, b, c) along with the exponent (γ_p) obtained by linear regression of log(P(*k*)) versus log(*k*) across the three mammals is shown in (d, e and f). Exponential approximation to (a, b and c) along with the exponent (γ_e) across the three mammals is shown in (g, h and i).

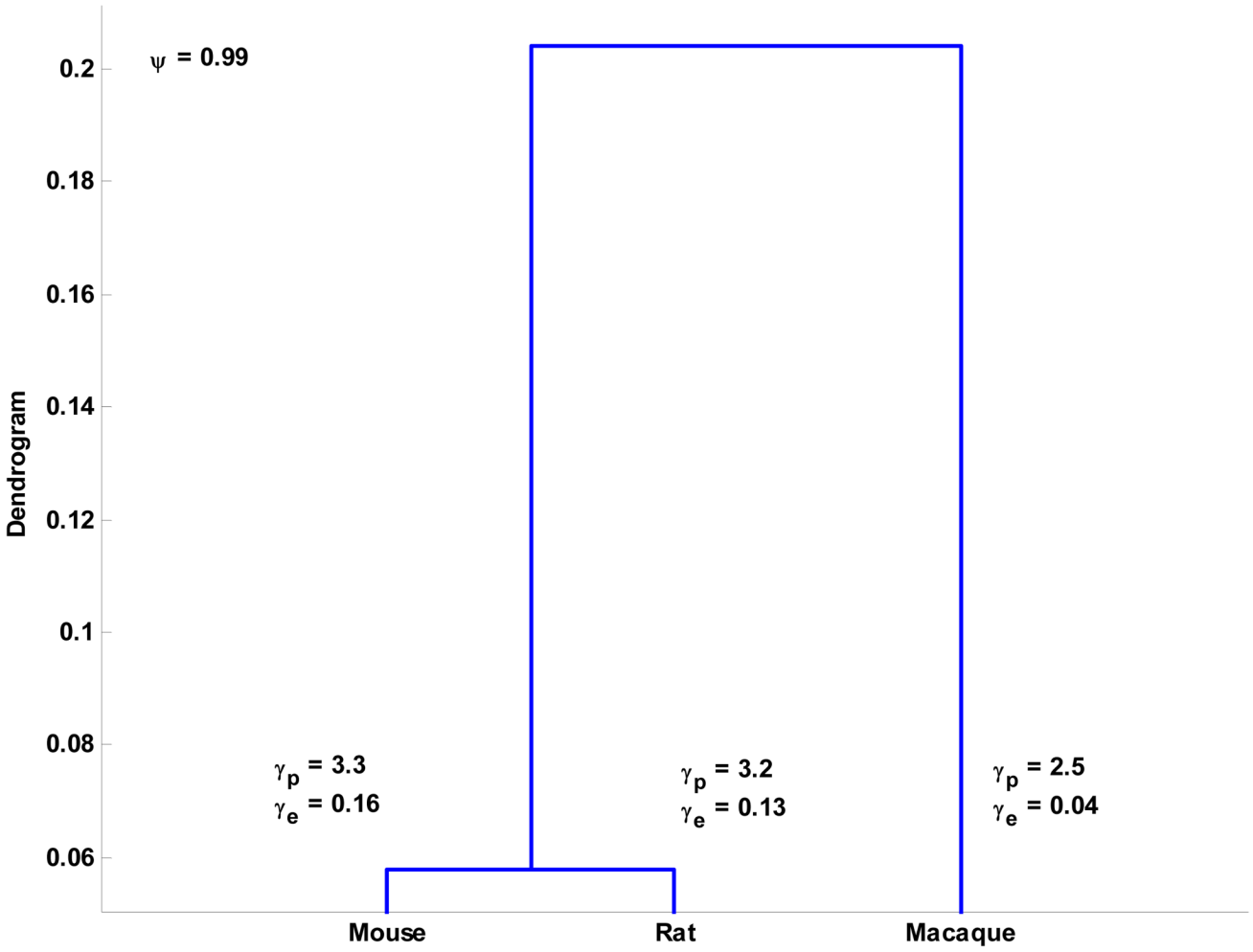

Figure 2.
Hierarchical clustering based on the 40 events common across the three mammals (Mouse, Rat and Macaques) using correlation metric and complete linkage reveals their phylogenetic proximity. This is also reflected by the similarity in the exponents obtained by power-law (γ_p) as well as exponential (γ_e) approximations to the distribution of the 40 common events, Fig. 1.

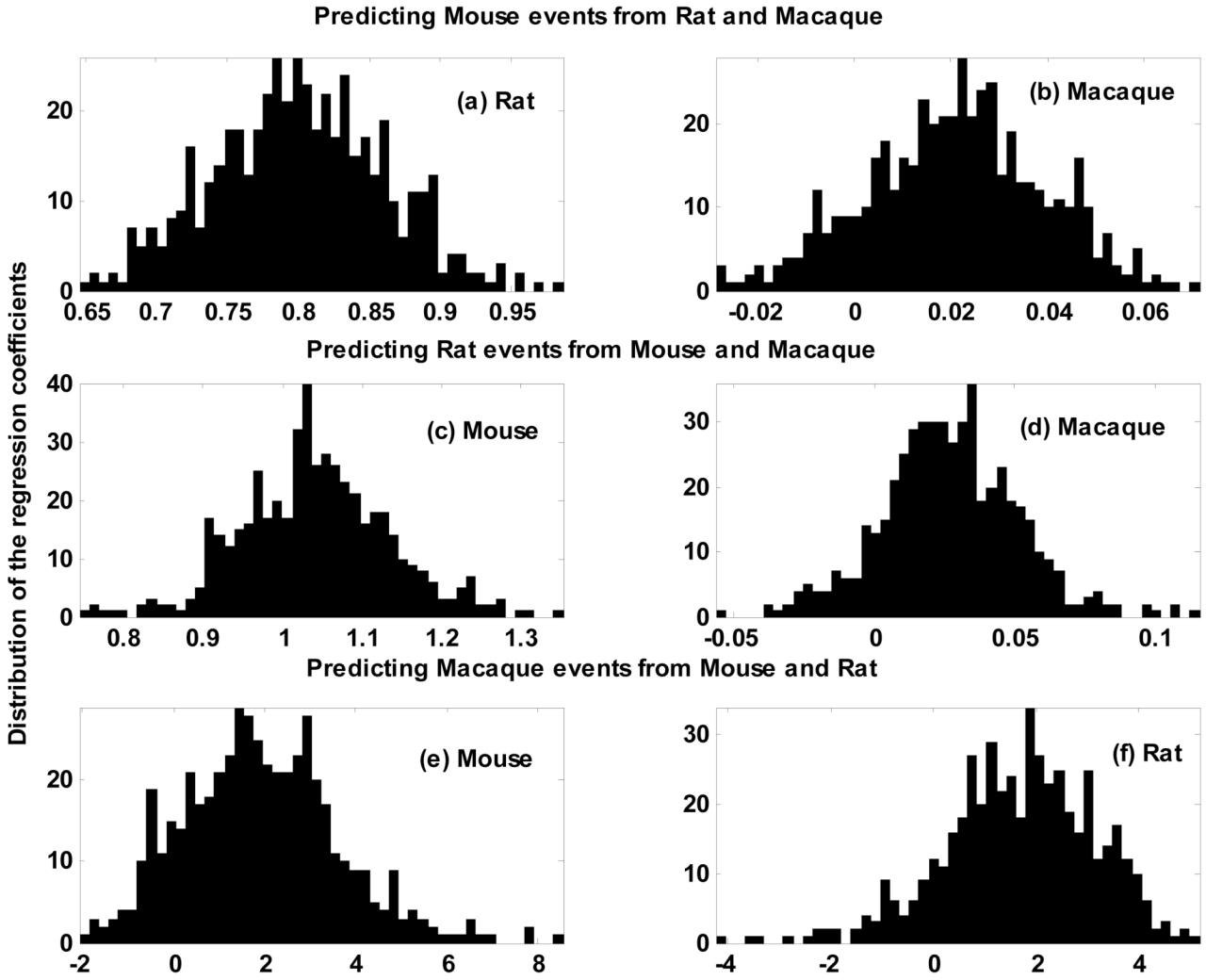

Figure 3.

Distribution of the regression coefficients across 500 independent bootstrap realizations, each consisting of 20 common events obtained by resampling without replacement from the 40 common events across the three species. Subplots (a) and (b) represent relative contribution of the rat and macaque in predicting mouse events. Subplots (c) and (d) represent relative contribution of the mouse and macaque in predicting rat events. Subplots (e) and (f) represent relative contribution of the mouse and rat in predicting macaque events.

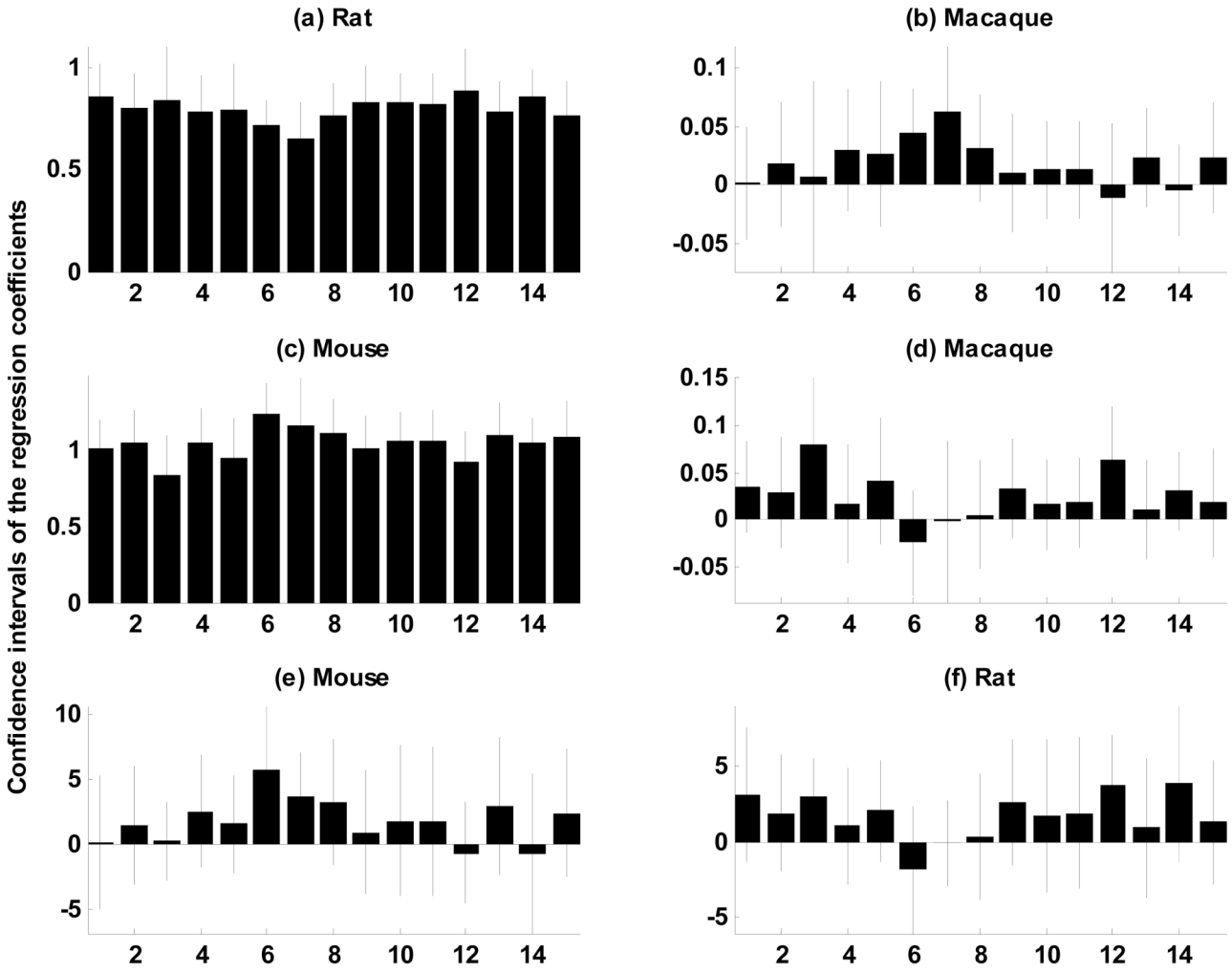

Figure 4.
The 95% confidence interval of the regression coefficient estimates across each of the cases in Fig. 3. Only 15 of the 500 bootstrap realizations are shown for clarity.

Table I

Neurodevelopmental event timings across Mouse, Rat and Macaque along with average values and standard deviations (CA1, CA2: hippocampal fields, cornu ammonis; dLGN: dorsal lateral geniculate nucleus; SC: superior colliculus; VC: visual cortex).

Events	Mouse	Rat	Macaque	Mean	SD
retinal ganglion cell generation - start of neurogenesis	10.5	11.5	30	17.3	11.0
subplate -start of neurogenesis	10	11.5	39.5	20.3	16.6
superficial SC laminae- start of neurogenesis	10.5	12.5	30	17.7	10.7
dLGN- start of neurogenesis	10.5	13.5	36	20.0	13.9
subplate - peak of neurogenesis	11	14	43	22.7	17.7
raphe complex - peak of neurogenesis	13.5	12	30	18.5	10.0
neurogenesis cortical layer VI - start (VC) of neurogenesis	11	13	45	23.0	19.1
Purkinje cells - peak of neurogenesis	10.5	14	39	21.2	15.5
medial forebrain bundle appears	13	13	35.5	20.5	13.0
dLGN - peak of neurogenesis	12	14	43	23.0	17.3
optic axons at chiasm of optic tract	13	15	36	21.3	12.7
fasciculus retroflexus appears	14	12.5	40	22.2	15.5
amygdala - peak of neurogenesis	12	15	38	21.7	14.2
superior colliculus - peak of neurogenesis	13	15	41	23.0	15.6
dLGN- end of neurogenesis	12.5	15.5	43	23.7	16.8
neurogenesis cortical layer V - start (VC) of neurogenesis	12	13.5	58.5	28.0	26.4
retinal ganglion cells - peak of neurogenesis	13	16	43	24.0	16.5
subplate - end of neurogenesis	12	15	48	25.0	20.0
neurogenesis cortical layer VI - peak (VC) of neurogenesis	12.5	16	53	27.2	22.4
septal nuclei - peak of neurogenesis	13	14	45	24.0	18.2
entorhinal cortex - peak of neurogenesis	13	14	48	25.0	19.9
caudoputamen – peak of neurogenesis	14	15	45	24.7	17.6
subiculum – peak of neurogenesis	13	16	48	25.7	19.4
parasubiculum – peak of neurogenesis	13.5	16	48	25.8	19.2
superficial SC laminae - end of neurogenesis	14	17.5	56	29.2	23.3
fornix appears	14	15	48	25.7	19.3
neurogenesis cortical layer V - peak (VC) of neurogenesis	13	16	70	33.0	32.1
presubiculum – peak of neurogenesis	13.5	17	48	26.2	19.0
neurogenesis cortical lamina VI - end (VC) of neurogenesis	13	15.5	65	31.2	29.3
neurogenesis cortical lamina IV - start (VC) of neurogenesis	15	15.5	70	33.5	31.6
CA 1, CA 2 - peak of neurogenesis	15	18	48	27.0	18.2
retinal amacrine cells - peak of neurogenesis	15	16	56	29.0	23.4
neurogenesis cortical layer V - end (VC) of neurogenesis	14	16.5	75	35.2	34.5
nucleus accumbens - peak of neurogenesis	16	19	45	26.7	15.9

Events	Mouse	Rat	Macaque	Mean	SD
neurogenesis cortical layer IV - peak (VC) of neurogenesis	17	17	80	38.0	36.4
retinal ganglion cell generation - end of neurogenesis	18.5	18.5	57	31.3	22.2
neurogenesis cortical layer II /III - peak (VC) of neurogenesis	15	18	90	41.0	42.5
neurogenesis cortical layer IV - end (VC) of neurogenesis	17	17.5	85	39.8	39.1
ipsi/contra segregation in LGN and SC	25.5	28.5	87	47.0	34.7
eye opening	30	36	123	63.0	52.0